Desalination and Water Treatment
www.deswater.com

doi: 10.1080/19443994.2015.1079251

57 (2016) 16445–16455
July

Taylor & Francis
Taylor & Francis Group

Nitrate adsorption by synthetic activated carbon magnetic nanoparticles: kinetics, isotherms and thermodynamic studies

Roshanak Rezaei Kalantary[a], Emad Dehghanifard[b], Anoushiravan Mohseni-Bandpi[c,*], Leila Rezaei[d], Ali Esrafili[a], Babak Kakavandi[e], Ali Azari[f]

[a]*Department of Environmental Health Engineering, School of Public Health, Iran University of Medical Sciences, Tehran, Iran, Tel. +98 2186704775; emails: rezaei.r@iums.ac.ir (R. Rezaei Kalantary), a_esrafily@yahoo.com (A. Esrafili)*
[b]*Department of Environmental Health Engineering, School of Public Health, Alborz University of Medical Sciences, Karaj, Iran, Tel. +98 2634643922; email: edehghanifard@gmail.com*
[c]*Department of Environmental Health Engineering, School of Public Health, Shahid Beheshti University of Medical Sciences, Tehran, Iran, Tel. +98 2122432040; email: anoushiravan.mohseni@gmail.com*
[d]*Department of Environmental Engineering, Islamic Azad University, Bandar Abbas Branch, Bandar Abbas, Iran, Tel. +98 7633665500; email: l_rezaei@gmail.com*
[e]*Department of Environmental Health Engineering, School of Health, Ahvaz, Jundishapur University of Medical Sciences, Ahvaz, Iran, Tel. +98 611 3738269; email: kakavandi.b@ajums.ac.ir*
[f]*Department of Environmental Health Engineering, School of Public Health, Tehran University of Medical Sciences, Tehran, Iran, Tel. +98 2186704775; email: ali_azari67@yahoo.com*

Received 16 November 2014; Accepted 28 July 2015

ABSTRACT

In this study, synthesized Fe_3O_4 magnetic nanoparticle (MNP) coated on powder activated carbon was applied for the adsorption of nitrate from aqueous solutions. This novel adsorbent was then characterized by Scanning electron microscopy, Transmission electron microscopy, X-ray diffraction, Fourier transform infrared spectroscope, and N_2 adsorption–desorption. Effects of variables such as pH, contact time, initial nitrate concentration, adsorbent concentration, and co-existing anions were all evaluated in detail. The adsorption of nitrate fitted best with the Langmuir isotherm ($R^2 = 0.993$) and pseudo-second-order kinetic models ($R^2 = 0.998$). The equilibrium time and the maximum monolayer capacity (Q_o) were determined to be 60 min and 57.1 mg/g, respectively (at pH 3). Thermodynamic studies revealed that the adsorption process of nitrate was spontaneous and endothermic. Moreover, the adsorption of nitrate followed the circumstantial interface in solid/liquid phases. Eventually, the activated carbon-Fe_3O_4 MNP (AC-Fe_3O_4 MNP) could be applied as a proper adsorbent for the removal of nitrate from aqueous solutions due to the advantages of high efficiency, rapid separation, and multiple usages.

Keywords: Adsorption; Nitrate; Equilibrium; Kinetics; Thermodynamics; Magnetic nanoparticles; Activated carbon

*Corresponding author.

1. Introduction

Nitrate, which is regarded as being one of the main concerns in water pollution, has caused a critical environmental problem worldwide due to its discharge into water resources [1,2]. Nitrate has been blamed for causing methemoglobinemia (also called blue baby syndrome), some cancers, and teratogenic effects [3]. Hence, WHO has set the maximum allowable concentration of nitrate in drinking at 50 mg/L [4].

Several methods have been applied for the nitrate removal from drinking water and wastewaters. They are all associated with physicochemical and biological processes like chemical reduction [5], electrocoagulation [6], adsorption [7,8], electrolysis [9], ion exchange resin [10], reverse osmosis [11], bacterial assimilation [12], etc. Adsorption, however, has been regarded as a promising process due to being economical and less production of sludge and fewer disposal problems [3].

Activated carbon (AC), a general adsorbent for removal of wide range of pollutants from water, has some important advantages such as special structure and high adsorption capacity which both have highlighted the AC application in many treatment plants. However, widespread application of AC in water purification has been a major concern due to some problems such as filtration, dispersion, turbidity, and high cost [13,14].

Magnetic separation method has been offered as an alternative when the above problems occur throughout the removal of pollutants from drinking water [15]. The magnetic adsorbents could be synthesized by jointing an adsorbent with iron oxides, which the latter could be of nanoscale particles [13,16]. Magnetic nanoparticles (MNPs) have the advantages of large surface area with remarkable active sites, which enhance the adsorption characteristics followed by a proper separation of the adsorbent from aqueous solution [17]. Moreover, MNPs could be easily recovered and reused for adsorption process. MNPs could also be employed *in situ*, and thus have been considered as the suitable material for on line separation. However, the strong tendency of MNPs toward agglomeration has still been a major concern for further application [18]. To overcome the above-mentioned problems, coating the MNPs with biocompatible, water-soluble, and nontoxic materials could be an effective choice.

The present work has focused on the removal of nitrate from water solutions using the synthesized Fe_3O_4-activated carbon MNPs (AC-Fe_3O_4 MNPs). The adsorbent displayed high efficiency for the adsorption of contaminants from aqueous effluents. And, when the adsorption was accomplished, the magnetic adsorbents were easily separated from the water solution by applying a magnetic field. Finally, the isotherms, kinetics, and thermodynamic parameters as well as the effect of co-existing anions on the adsorption efficiency of nitrate using AC-Fe_3O_4 MNPs were fully investigated.

2. Materials and methods

2.1. Chemicals

Potassium nitrate (KNO_3), nitric acid (HNO_3 65%), ferric nitrate ($Fe(NO_3)_3{\cdot}9H_2O$), powder activated carbon (PAC), natrium chloride (NaCl), hydrochloric acid fuming (HCl 37%), magnesium chloridehexahydrate ($MgCl_2{\cdot}6H_2O$), natrium carbonate (Na_2CO_3), and natriumsulfate (Na_2SO_4) were all of analytical grade and purchased from Merck.

2.2. Synthesis and characterization of AC-Fe_3O_4 MNPs

The synthesis of AC-Fe_3O_4 MNPs was conducted based on a chemical co-precipitation method according to our previous study [16]. Briefly, an specific amount of AC was impregnated by nitric acid (63%) for 3 h at 80˚C (using an ultrasonic bath) in order to make the adsorbent hydrophilous. Then, 5 g of the prepared powder was impregnated by a 200 mL of aqueous solution containing Fe $(NO_3)_3{\cdot}9H_2O$ and placed in ultrasonic vibration for a 1 h at 80˚C. Then, the adsorbent was heated using a 750˚C furnace within 3 h under nitrogen gas to form AC-Fe3O4 MNPs. Finally, the synthesized magnetized adsorbent washed with deionized water and dried at 105˚C and kept in a desiccators. The morphology of the exterior surface of synthesized AC-Fe_3O_4 MNPs was observed with a scanning electron microscope (SEM, PHILIPS, XL-30) equipped with energy dispersive X-ray microanalysis. The adsorbent was also analyzed by transmission electron microscopy (TEM, PHILIPS, EM 208) to determine the mean particle size of the synthesized adsorbent under 200 kV. X-ray diffraction (XRD) pattern of the adsorbent was performed to identify the crystalline structure of the adsorbent using Quantachrome, NOVA 2000 diffractometer. Mono chromatized Cu-kα radiation was employed in diffractometery. Operation of XRD was done using Cu-kα radiation, $\lambda = 1.54$ Å at 25˚C. The Fourier Transform Infrared (FTIR) spectroscopy (Bruker-VERTEX 70) was applied in order to determine the functional groups on the surface of the adsorbent over 400–4,000 cm^{-1}. The specific surface area of the adsorbent was measured using a nitrogen

adsorption–desorption technique on the basis of the Brunauer–Emmet–Teller (BET) isotherm model.

In order to determine the point of zero charge of the adsorbent (pH_{pzc}), a known amount of AC-Fe_3O_4 MNPs was added to 0.01-M NaCl solution. The samples were stirred at 200 rpm for 48 h and then the pH values were measured after the removal of the adsorbent. The pH_{pzc} value was determined using a plot of initial pH vs. ΔpH ($\Delta pH = pH_{initial} - pH_{final}$).

2.3. Removal of nitrate from aqueous solution by AC-Fe3O4 MNPs adsorbent

The stock solution of nitrate (1,000 mg/L) was prepared by dissolving the required amounts of KNO_3 in distilled water. The adsorption experiments were conducted in a batch mode (100 mL Erlenmeyer flasks) on a shaker (Bioteck) at 180 rpm. Optimization of pH and contact time was performed within the range of 3.0–11.0 and 0–180 min, respectively. Then, the adsorption of nitrate under different concentration range (50–300 mg/L) and different amounts of adsorbent (0.5–2 g/L) was studied, respectively.

A magnet with an intensity of 1.3 T (5 cm × 5 cm × 4 cm) was used for magnetic separation of the adsorbent from the aqueous solution. UV–visible spectrophotometer (CECIL CE7400) for measurement of the residual concentration of nitrate was employed.

The amount of adsorbed nitrate by the AC-Fe_3O_4 MNPs was determined by Eq. (1):

$$q_e = (C_0 - C_e)V/m \tag{1}$$

where q_e is the adsorption capacity of AC-Fe_3O_4 MNPs adsorbent at a given time t (mg/g), V is the volume of solution (L), m is the mass of adsorbent (g) and C_0 and C_e (mg/L) are the initial and equilibrium concentration of nitrate, respectively.

2.4. Isotherms, kinetics, and thermodynamics of the adsorption process

In adsorption process, the study of equilibrium adsorption isotherm is the basis for the modeling of an adsorption system. The Langmuir, Freundlich, and Temkin isotherm were all applied for the analysis of adsorption data and represented by the following equations, respectively:

$$\frac{C_e}{q_e} = \frac{1}{b\,Q_o} + \frac{C_e}{Q_o} \tag{2}$$

$$\log q_e = \log k_f + \frac{1}{n}\log C_e \tag{3}$$

$$q_e = \frac{RT}{b}\ln(K_T C_e) \tag{4}$$

where q_e (mg/g) and b (L/mg) are the solid-phase equilibrium concentration of nitrate and the Langmuir adsorption constant, respectively. C_e (mg/L) is the equilibrium concentration of nitrate in the solution [19]. k_f (L/mg) is the adsorption capacity and n (unitless) is the intensity of the Freundlich isotherm which reveals the type of adsorption as follows: favorable (2–10); moderately difficult (1–2); or poor adsorption ($n < 1$). In order to describe the principal properties of the Langmuir isotherm, a term R_L ($R_L = 1/(1 + bC_0)$)—a dimensionless separation factor—was considered. This factor may be varied between unfavorable ($R_L > 1$), favorable ($0 < R_L > 1$), irreversible ($R_L = 0$), and linear adsorption ($R_L = 1$) [20]. In the Temkin isotherm, R is the universal gas, b (J/mol) and K_T (L/mg) are Temkin constants [21].

Three kinetic models (pseudo-first-order [22], pseudo-second-order [23] and intraparticle diffusion [24]) were applied for the analysis of adsorption of nitrate onto AC-Fe_3O_4 MNPs expressed by the following equations:

$$\ln(q_e - q_t) = \ln q_e - k_1 t \tag{5}$$

$$\frac{t}{q_t} = \frac{1}{k_2 q_e^2} + \frac{1}{q_e}t \tag{6}$$

$$q_t = k_i t^{0.5} + C_i \tag{7}$$

k_1 (1/min) and K_2 (g/(mg min)) are the rate constant of the first- and second-order adsorption, respectively. In Eq. (7), the intraparticle diffusion (k_i mg/g $min^{0.5}$) represents the model constant. The k_i is directly related with the rate of adsorption process controlled by intraparticle diffusion. C_i (mg/g) is a constant value depicting the boundary layer effects. If the curve (q_t vs. $t^{0.5}$) was multilinearity, it could imply that two or more controlling steps might affect the adsorption process [25]. If C_i was equal to zero ($C_i = 0$), intraparticle diffusion would the only rate-determining step. In contrast, $C_i \neq 0$ values suggest the adsorption process is rather complicated and involved in more than one diffusive resistance process [16].

Fundamental thermodynamic parameters including standard enthalpy (ΔH°), standard free energy (ΔG°), and standard entropy (ΔS°) were all measured for thermodynamic studies. Van't Hoff plots were

employed for the calculation of ΔH° and ΔS° based on the following equations:

$$\ln k_c = -\frac{\Delta H^\circ}{RT} + \frac{\Delta S^\circ}{R} \quad (8)$$

where k_c (L/g) is the distribution coefficient and T (K) is the solution temperature. The ΔG° value was measured based on the following expression:

$$\Delta G^\circ = -RT \ln k_c \quad (9)$$

2.5. Reusability of the adsorbent

Reusability experiments were carried out in order to determine the potential of AC-Fe_3O_4 MNPs for multiple usages based on the adsorption–desorption ratio of nitrate. Desorption process of nitrate from the used adsorbent was investigated using an aqueous solution of HCl (0.1 M). The used adsorbent was placed in the desorption solution and shaken for 4 h at 30°C. Then, the supernatant was analyzed for measuring the nitrate concentration. Desorption ratio was calculated by and the ratio of final concentration of nitrate to concentration of nitrate in the desorption solution [26].

2.6. Effects of co-existing anions

Water resources contain different anions like chloride, carbonate, and sulfate which may interfere the nitrate adsorption onto AC-Fe_3O_4 MNPs. Hence, the synthetic solution was prepared at different concentration of existing anions present in natural waters and their reciprocal effects on the adsorption of nitrate were investigated. Then, the removal efficiency of nitrate in the synthetic solution (1.5 mM of co-existing anions such as CO_3^{2-}, SO_4^{2-}, and Cl^-) was determined.

3. Results and discussion

3.1. Characterization of AC-Fe_3O_4 MNPs adsorbent

The synthesized adsorbent was characterized using various instrumental techniques including SEM, XRD, BET, and TEM. The SEM micrograph of AC-Fe_3O_4 MNPs representing the surface morphology of the synthesized adsorbent is illustrated in Fig. 1. As depicted, it is highly porous with the following features: almost regular texture, a relatively smooth surface, and low number of cavities. The porous nature of the synthesized MNPs is an implication of large surface area and high adsorption capacity. Formation of the magnetic AC was confirmed by the presence of several monodisperse Fe_3O_4 MNPs (about 10 nm diameter) embedded in AC pores.

XRD analysis was performed to examine the crystal structure of the synthesized adsorbent. The typical XRD pattern of AC-Fe_3O_4 MNPs is shown in Fig. 2. The appearance of a broad peak at $2\theta = 34.4^\circ$ could be interpreted as the evidence for the presence of Fe_3O_4 crystalline phase [27,28]. The main peak at $2\theta = 25.1^\circ$ corresponds to carbon [29]. Thus, the findings from the XRD analysis strongly support the impregnation of MNPs on the surface of AC.

The specific surface area of AC-Fe_3O_4 MNPs was determined to be 650–700 m^2/g-partially less than that of used PAC (733 m^2/g) [17]. This fall could be attributed to the occupation of almost the entire pores of PAC with MNPs resulting in less accessible pores. This result had an agreement with the related previous works. The N_2 adsorption–desorption isotherms, volume, and pore size distribution for AC-Fe_3O_4 MNPs by applying the methods of BET were shown in Fig. 3. It exhibited the type-IV isotherm for the prepared adsorbent as categorized by International Union of Pure and Applied Chemistry (IUPAC), which indicates that the adsorbent structure is typically mesoporous [30]. Moreover, the mean pore size of the adsorbent based on IUPAC classification corresponds to the class of mesopores ($2 < d < 50$ nm) [31].

The TEM analysis of the adsorbent (Fig. 4) clearly reveals the fine Fe_3O_4 particles with diameter of less than 50 nm. Accordingly, Fe_3O_4 nanoparticles are of a cubic structure. These results also confirmed the successful synthesis of Fe_3O_4 crystals on the AC surface. The FTIR spectrum of AC-Fe3O4 MNPs, before, and after the adsorption of nitrate, is shown in Fig. 5. The broad band at 3,414 cm^{-1} and the peak at 1,574 cm^{-1} could be related to the stretching and bending vibration of adsorbed water, and the peak at 1,150 cm^{-1} could be assigned to the bending vibration of hydroxyl group on metal oxide (Fe–O) [32,33]. The band at 1,590 cm^{-1} is attributed to the coupling of the unbalanced vibration modes of the oxygen atoms. Moreover, the band at 579 cm^{-1} was assigned to the stretching vibration and the tensional vibration of Fe–O bonds in the tetrahedral and octahedral sites of Fe_3O_4 [34]. As can be seen, after the sorption of nitrate, the new band at 1,389 cm^{-1} was appeared. Furthermore, the intensity of peak at 1,150 cm^{-1} fell with an increase in nitrate concentration which means that the hydroxyl groups on the surface of adsorbent were involved in the adsorption of nitrate [13].

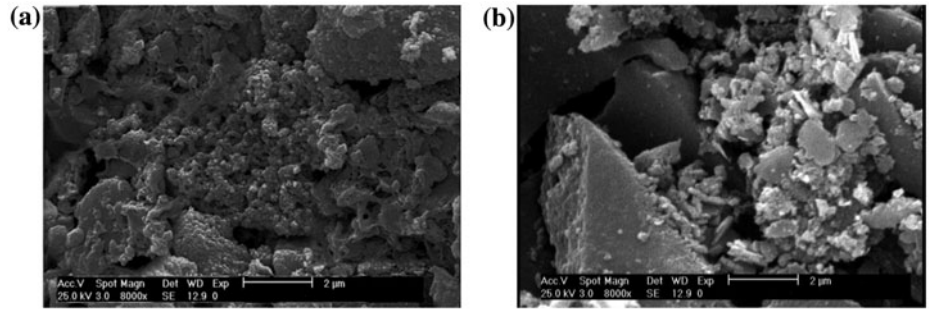

Fig. 1. SEM image of synthesized AC-Fe_3O_4 MNPs adsorbent: (a) raw AC and (b) AC-Fe_3O_4 MNPs.

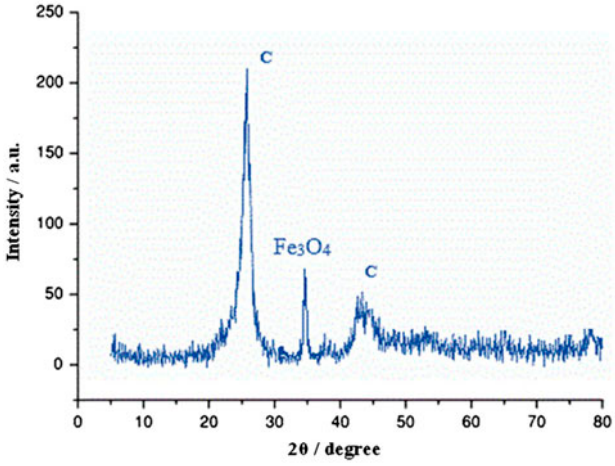

Fig. 2. XRD curve of synthesized AC-Fe_3O_4 MNPs adsorbent.

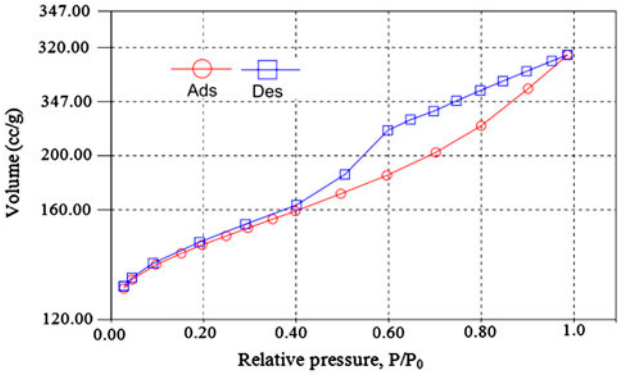

Fig. 3. N_2 adsorption/desorption isotherms for AC-Fe_3O_4 MNPs.

The pH_{pzc} for the synthesized adsorbent was measured to be 5.5. It is worth noting that pH_{PZC} was considered for the explanation of pH effect on the ions adsorption.

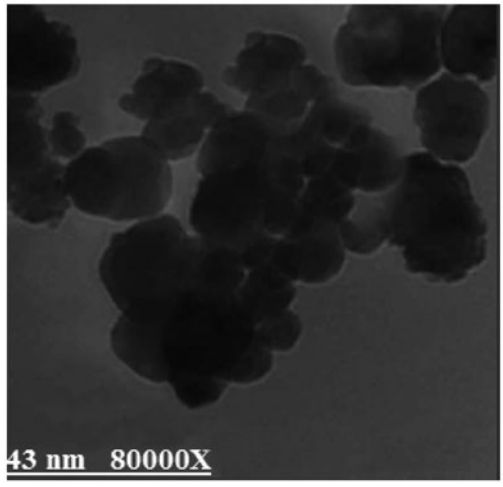

Fig. 4. TEM image of synthesized AC-Fe_3O_4 MNPs adsorbent.

3.2. Effect of pH

pH has an important role in the adsorption process of nitrate mainly on the adsorption capacity. Fig. 6 shows that the maximum adsorption efficiency of nitrate obtained was about 58.2% at pH 3.0. However, the adsorption efficiency dropped sharply to 8.2% as the pH was raised to 11.0. Öztürk and Bektaş reported that the maximum adsorption of nitrate on the AC (about 92%) occurred at pH 2.0 due to an increase in the number of positively charged sites on the surface of AC [35]. At lower pH, the surface of adsorbent was dominantly charged with the positive ions (protons). Accordingly, the adsorption of nitrate was promoted due to the electrostatic attraction.

In a further related study, Xu et al. reported that the optimum pH range for removal of nitrate using the stratified wheat straw resin was within 6.0–8.0 (35.3 mg/g adsorbent). This could be explained due to the fact that the state of functional groups on these

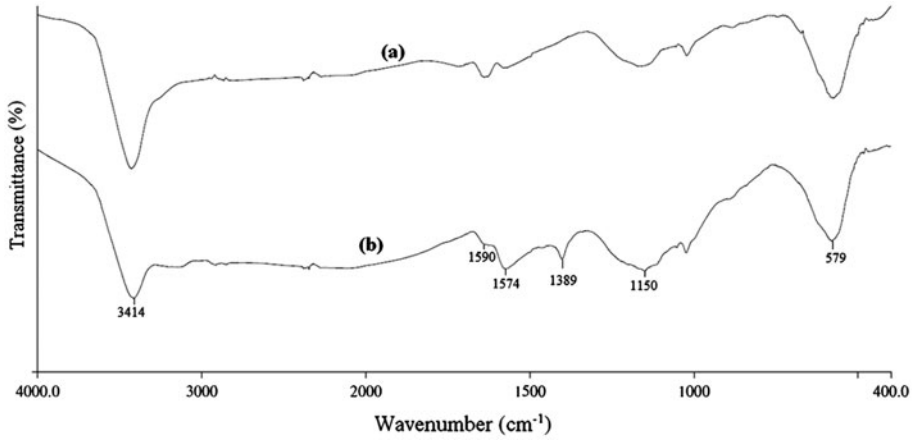

Fig. 5. FTIR spectra of synthesized AC-Fe_3O_4 MNPs adsorbent (a) before nitrate adsorption and (b) after nitrate adsorption.

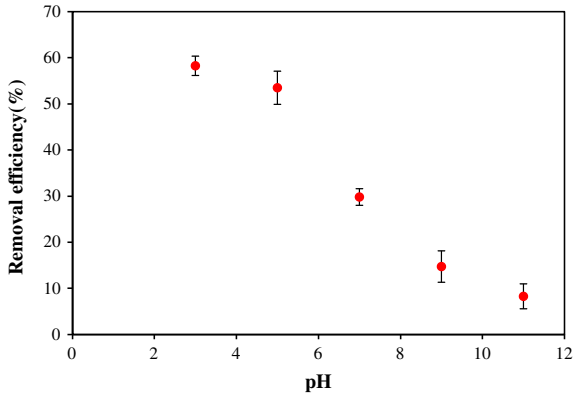

Fig. 6. Effect of pH on the adsorption efficiency of nitrate by synthesized AC-Fe_3O_4 MNPs adsorbent (conditions: C_0 = 100 mg/L, adsorbent dose = 1 g/L, contact time = 120 min and T = 25 ± 1°C).

adsorbents is always affected by the pH_{pzc} leading to the lower uptakes in basic or acidic influents [3].

The adsorption mechanism for anions was specific and/or non-specific. The specific adsorption was based on ligand exchange reactions (replacement of OH groups of the adsorbent with anions), while the coulombic forces played a vital role in nonspecific adsorption, which was heavily dependent on the pH_{PZC} of the adsorbent [36]. In the current study, the pH_{PZC} obtained for the synthesized AC-Fe_3O_4 MNPs was about 6.8 and the best removal efficiency of nitrate was achieved at pH 3.0. It could be concluded that the mechanism of nitrate adsorption followed a non-specific adsorption pattern.

3.3. Effect of contact time and kinetics of adsorption

Contact time is regarded as being one of the main parameters affecting the adsorption efficiency. As demonstrated in Fig. 7, the maximum removal efficiency of nitrate adsorption was achieved after 60 min which was about 57.4%. However, longer contact times did not significantly improve the adsorption of nitrate. Therefore, the equilibrium time for the adsorbent was set at 60 min for initial concentration of nitrate (100 mg/L N) and the adsorbent (1 g/L). This phenomenon could be explained by the fact that a great numbers of active sites could lead to a fast adsorption rate of nitrate on synthesized AC-Fe3O4

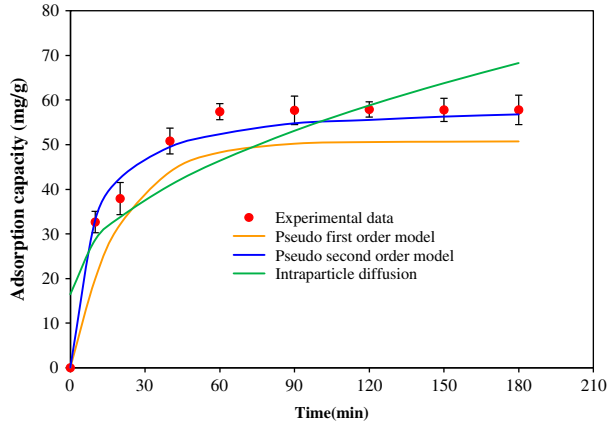

Fig. 7. Effects of contact time on the adsorption efficiency of nitrate by synthesized AC-Fe_3O_4 MNPs adsorbent (conditions: pH 3, C_0 = 100 mg/L, adsorbent dose = 1 g/L and T = 25 ± 1°C).

MNPs. However, at longer contact times, the availability of adsorbent active sites for the adsorption of nitrate ions was reduced [28]. In a further related study, Cho et al. reported the equilibrium time of 90 min for the removal of nitrate by CPM-GAC (cationic polymer-modified granular activated carbon) from aqueous solutions [1].

The pseudo-first, pseudo-second-order kinetics, and intraparticle diffusion were applied to analyze nitrate adsorption on the AC-Fe_3O_4 MNPs in terms of adsorption rate. Table 1 presents the values of kinetic model for nitrate adsorption onto AC-Fe_3O_4 MNPs. The correlation coefficient (R^2) 0.972, 0.998, and 0.774 were obtained for pseudo-second, pseudo-second-order, and intraparticle diffusion kinetic model, respectively. This suggests that the adsorption by AC-Fe_3O_4 MNPs fitted best to pseudo-second-order-kinetic model which may be due to the adsorption dependency on the amounts of nitrate adsorbed on the Fe_3O_4 MNPs at equilibrium condition [28]. Furthermore, a good agreement between the calculated q_e and the experimental q_e was observed in the pseudo-second-order model. Hence, it could be concluded that the adsorption of nitrate followed the chemisorption mechanism, which incorporates the exchange or sharing of electrons between nitrate and the binding sites on the AC-Fe_3O_4 MNPs [37].

In a similar related study, Demiral and Gündüzoglu reported that the adsorption of nitrate by AC prepared from sugar beet bagasse fitted best to the pseudo-second-order kinetic model ($R^2 = 0.998$) [38]. In a further related study, Wan et al. found out that both nitrate and nitrite adsorption followed the pseudo-second-order rather than pseudo-first model using calcined hydrotalcites adsorbent [39].

According to Table 1, the value of C_i was measured to be 16.43 mg/g indicating that intraparticle diffusion was not the only controlling step for nitrate adsorption on the AC-Fe_3O_4 MNPs, and to some extent the process was controlled by boundary layer diffusion [16,25]. The low R^2 value (0.66) of the intraparticle diffusion model also revealed that the pore diffusion was not the rate-controlling step.

3.4. Effect of different concentrations of adsorbent and nitrate

At equilibrium time of 60 min and the optimum pH of 3.0, the effects of adsorbent and nitrate concentration on the adsorption efficiency were investigated in the range of 0.5–2 g/L and 50–300 mg/L, respectively. As shown in Fig. 8, by increasing AC-Fe_3O_4 MNPs dosage from 0.5 to 2 g/L, the adsorption percentage of nitrate increased from 23.1 to 90.4% (Table 2). This could be explained by the fact that an increase in the adsorbent dose may increase the accessibility of the active sites on the pores of the AC-Fe_3O_4 MNPs for the nitrate ions, which leads to an enhancement in the removal efficiency [16]. Since the nitrate removal percentage of 56.7% was obtained in the presence of AC-Fe_3O_4 MNPs 1 g/L, which is still less than the maximum allowable concentration of nitrate in drinking water (50 mg/L), 1 g/L of AC-Fe_3O_4 MNPs was selected as the optimal dosage of the adsorbent for the adsorption process. Fig. 8 also indicates that the adsorption percentage of nitrate was decreased from 77.3 to 18.7% as an initial nitrate concentration was increased from 50 to 300 mg/L (on 1 g/L of AC-Fe_3O_4 MNPs). This was probably due to a fixed number of active sites available for nitrate on the adsorbent [14]. Similar behavior was observed for nitrate adsorption on other adsorbents as reported in the literature [1,38,40].

3.5. Adsorption isotherm

The study of adsorption isotherm has been considered as an important view point for theoretical and practical design of adsorption systems [3]. Therefore, the determination of proper correlation of the equilibrium data is essential for optimization of a design for an adsorption system. In this study three models, namely the Langmuir, Freundlich, and Temkin were employed as common isotherms for analysis of adsorption data. The Temkin isotherm proposed a linear reduction of sorption energy as the completion of sorption increased. The heat of adsorption for all the

Table 1
Values of kinetic model parameters of nitrate adsorption on AC-Fe_3O_4 MNPs

Pseudo-first-order				Pseudo-second-order		Intraparticle diffusion		
$q_{e,cal}$ (mg/g)	K (min^{-1})	R^2	$q_{e,cal}$	K_2 (g/mg min)	R^2	k_i	C_i	R^2
50.8	0.05	0.972	59.17	0.002	0.998	3.86	16.43	0.774
$q_{e,exp}$(mg/g)				**57.4**				

Note: q_e showed the capacity of the adsorbent in the pseudo-second-order which the adsorption process was best fitted to this model.

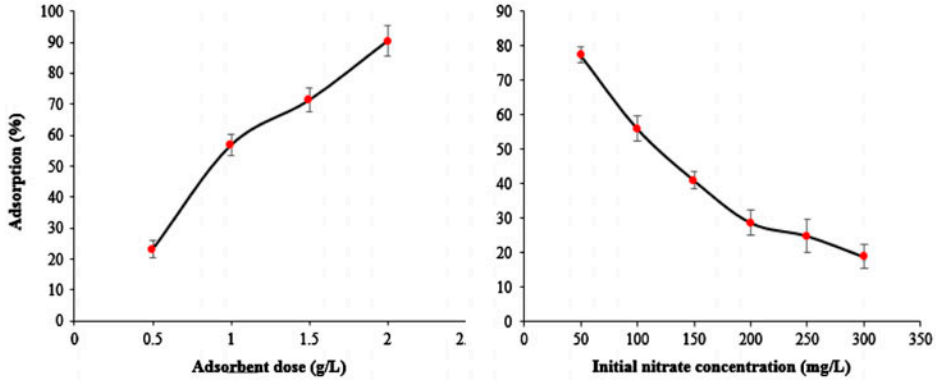

Fig. 8. The effect of various concentrations of nitrate and AC-Fe_3O_4 MNPs on the adsorption percentage (conditions: pH 3.0, contact time = 60 min and T = 25 ± 1˚C).

Table 2
Comparison of the adsorption performance of different adsorbents in removal of nitrate anion

Adsorbent	pH	q_m (mg/g)	Refs.
AC-Fe3O4 MNPs	3	57.4	
Granular-activated carbon	6.5	26	[1]
Powdered-activated carbon	3	27.55	[38]
Ammonium-functionalized MCM-48	5	34	[40]

molecules in the layer decreased linearly with the coverage due to the adsorbent interactions. The adsorption was characterized by a uniform distribution of binding energy.

As shown in Table 3, the correlation coefficients of the Langmuir isotherm were found out to be 0.993 at all selected temperatures. As the temperature increased from 20 to 45˚C, the maximum adsorption capacity (q_e) increased from 57.1 to 68.9 mg/g. R_L, a dimensionless equilibrium parameter, was considered as an additional analysis in the Langmuir equation. The desirable adsorption was achieved when the average R_L value (different initial nitrate concentrations) fell between 0 and 1 [38]. The results also revealed that the Freundlich correlation coefficients were significantly lower than those of Langmuir isotherm. This implies that the nitrate adsorption follows a monolayer pattern with a homogenous adsorption patch. According to the previous studies, the nitrate

Table 3
Parameters of adsorption equilibrium isotherms for AC-Fe_3O_4 MNPs

Isotherms	Temperature (˚K)	Constants			
Langmuir		Q_o	b	R_L	R^2
	293	57.1	0.185	0.973	0.993
	308	64.5	0.160	0.77	0.993
	318	68.9	0.156	0.4	0.993
Freundlich			K_f	n	R^2
	293		30.84	7.69	0.713
	308		31.56	7.14	0.716
	318		31.9	6.66	0.754
Temkin			K_T	b	R^2
	293		81.11	387	0.7
	308		40.1	341.4	0.69
	318		31	330.5	0.73

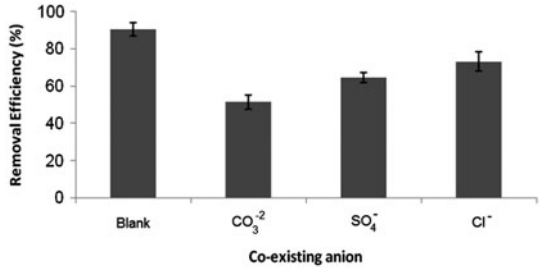

Fig. 9. Effects of Co-existing anion on the adsorption efficiency of nitrate by synthesized AC-Fe_3O_4 MNPs adsorbent (1.5 mM) (conditions: pH 3, C_0 = 100 mg/L, adsorbent dose = 1 g/L and T = 25 ± 1˚C).

Table 4
Thermodynamic parameters of nitrate adsorption by AC-Fe_3O_4 MNPs adsorbent

Temperature (K)	ln k_1	ΔG° (kJ/mol)	ΔH° (kJ/mol)	ΔS° (kJ/mol K)
293	1.22	−2.98	88.5	0.37
308	1.37	−3.51		
318	1.48	−3.92		

adsorption on AC obeyed the Langmuir isotherm [36,38,41]. The results also showed that the R_L values for adsorption of nitrate by synthesized AC-Fe_3O_4 MNPs adsorbent were between 0.4 and 0.973, implying that the adsorption of nitrate was favorable. The q_e and the Langmuir constant (b) of the AC-Fe_3O_4 MNPs adsorbent (at 20˚C) were obtained to be 57.1 mg/g and 1.05 L/mg, respectively. This desirable process was also confirmed by the Freundlich exponent n; n values were located between 1 and 10 under all studied temperatures [38,42].

3.6. Thermodynamic studies

Temperature has been considered as an important parameter affecting the adsorption efficiency. As demonstrated in Table 4, the ΔG° values at selected temperatures (20, 35, and 45˚C) were negative; while, the corresponding ΔH° values were positive. The negative values of ΔG° imply that the adsorption process of nitrate is of spontaneous nature, while the positive ΔH° values are an indicator of endothermic adsorption. Moreover, the adsorption process of nitrate was favorable at higher temperatures due to the fall of $-\Delta G^\circ$. The ΔH° value was determined to be 88.5 kJ/mol (between 80 and 200 kJ/mol) indicating that the transportation of nitrate ions from the aqueous solution to the AC-Fe_3O_4 MNPs surface occurred chemically [43]. This finding was also consistent with the results obtained from the study of the adsorption kinetics. The positive values of ΔS° indicate that the adsorption of nitrate was dependent on AC-Fe_3O_4 MNPs adsorbent and circumstantial interface in solid/liquid phases.

3.7. Effect of co-existing ions

Anions present in natural waters may compete with nitrate adsorption [39]. The presence of common anions in water such as, CO_3^{2-}, SO_4^{2-}, and Cl^- may affect the adsorption efficiency of nitrate on AC-Fe_3O_4 MNPs. As demonstrated in Fig. 9, the presence of those anions (1.5 mM) decreased the adsorption capacity of nitrate. Their impact on the nitrate adsorption was in the following order: $CO_3^{2-} > SO_4^{2-} > Cl^-$. Anions have electron affinity toward AC-Fe_3O_4 MNPs contesting with the target anion (nitrate) in the adsorption process. Several studies reported that the multivalent anions had more adsorption tendency compared with mono charge ones, which could be attributed to high ionic strength [39,44]. Therefore, divalent anions like CO_3^{2-} and SO_4^{2-}could conquer on nitrate in the adsorption process. Moreover, the presence of Cl^- decreased the nitrate adsorption less than expected due to having a shorter anion radius, although Cl^- has the same charge capacity as nitrate.

3.8. Reusability potential of the adsorbent

Desorption could be regarded as a substantial process because of the importance of economical issues. Aqueous solutions containing HCl (0.1 M) were used for measurement of desorption efficiency of the applied adsorbent. Results showed that the desorption efficiency of nitrate using 0.1 M HCl was about 98.9%. The adsorption–desorption experiment was repeated 10 times using the same adsorbent. As shown in Fig. 10, a slight decrease in the adsorption capacity of AC-Fe3O4 MNPs throughout the regeneration cycles was observed

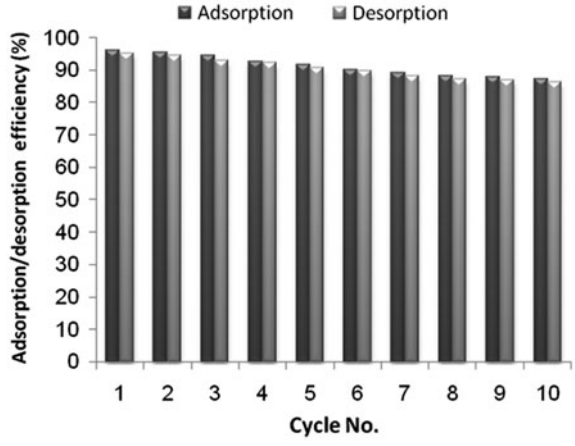

Fig. 10. Adsorption–desorption cycles for nitrate adsorption by synthesized AC-Fe_3O_4 MNPs adsorbent(conditions: C_0 = 50 mg/L, adsorbent dose = 1 g/L, adsorption contact time = 240 min, 0.1 M HCl and T = 25 ± 1˚C).

(from 96.1 to 87.5%). Considering the reusability of the adsorbent, the results also showed that AC-Fe_3O_4 MNPs had high capacity for adsorption, which makes the adsorbent to be reused nearly 10 times without a significant loss in the adsorption efficiency [45,46].

4. Conclusion

The adsorption process is an appropriate method for the removal of nitrate from drinking water. The synthesis of AC-Fe_3O_4 MNPs adsorbent was prosperously applied to remove nitrate from the aqueous solutions. The pseudo-second-order and the Langmuir isotherm model fitted best to the kinetics of adsorption indicating that the adsorption of nitrate followed the homogeneous chemisorption process. The AC-Fe_3O_4 MNP adsorbent was easily synthesized and regenerated and then applied as a reversible adsorbent for highly efficient removal of nitrate. The study also showed that the application of the synthetic adsorbent in larger scales could be a proper economical choice concerning the removal of nitrate from water. The magnetic characteristics of the adsorbent improved its reusability for multiple usages, which reduces the cost and the time required for the removal of nitrate.

Acknowledgment

Authors highly appreciate Bandar Abbas Branch, Islamic Azad University (BAIAU) for the support of this study.

References

[1] D.W. Cho, C.M. Chon, Y. Kim, B.H. Jeon, F.W. Schwartz, E.S. Lee, H. Song, Adsorption of nitrate and Cr(VI) by cationic polymer-modified granular activated carbon, Chem. Eng. J. 175 (2011) 298–305.
[2] X. Xu, B.-Y. Gao, Q.Y. Yue, Q.Q. Zhong, Preparation of agricultural by-product based anion exchanger and its utilization for nitrate and phosphate removal, Bioresour. Technol. 101 (2010) 8558–8564.
[3] X. Xu, B. Gao, X. Tan, X. Zhang, Q. Yue, Y. Wang, Q. Li, Nitrate adsorption by stratified wheat straw resin in lab-scale columns, Chem. Eng. J. 226 (2013) 1–6.
[4] World Health Organization, Guidelines for Drinking Water Quality, fourth ed., World Health Organization, Geneva, Switzerland, 2011.
[5] A. Devadas, S. Vasudevan, F. Epron, Nitrate reduction in water: Influence of the addition of a second metal on the performances of the Pd/CeO_2 catalyst, J. Hazard. Mater. 185 (2011) 1412–1417.
[6] J. Lakshmi, G. Sozhan, S. Vasudevan, Recovery of hydrogen and removal of nitrate from water by electrocoagulation process, Environ. Sci. Pollut. Res. 20 (2013) 2184–2192.
[7] R. Katal, M.S. Baei, H.T. Rahmati, H. Esfandian, Kinetic, isotherm and thermodynamic study of nitrate adsorption from aqueous solution using modified rice husk, J. Ind. Eng. Chem. 18 (2012) 295–302.
[8] P. Ganesan, R. Kamaraj, S. Vasudevan, Application of isotherm, kinetic and thermodynamic models for the adsorption of nitrate ions on graphene from aqueous solution, J. Taiwan Inst. Chem. Eng. 44 (2013) 808–814.
[9] S. Vasudevan, M.A. Oturan, Electrochemistry: As cause and cure in water pollution—An overview, Environ. Chem. Lett. 12 (2014) 97–108.
[10] M.D. Gupta, P. Loganathan, S. Vigneswaran, Adsorptive removal of nitrate and phosphate from water by a purolite ion exchange resin and hydrous ferric oxide columns in series, Sep. Sci. Technol. 47 (2012) 1785–1792.
[11] V. Goncharuk, V. Osipenko, M. Balakina, D. Kucheruk, Water purification of nitrates by low-pressure reverse osmosis method, J. Water Chem. Technol. 35 (2013) 71–75.
[12] P. Ayyasamy, S. Rajakumar, M. Sathishkumar, K. Swaminathan, K. Shanthi, P. Lakshmanaperumalsamy, S. Lee, Nitrate removal from synthetic medium and groundwater with aquatic macrophytes, Desalination 242 (2009) 286–296.
[13] B. Kakavandi, A. Jonidi Jafari, R. Rezaei Kalantary, S. Nasseri, A. Ameri, A. Esrafily, Synthesis and properties of Fe_3O_4-activated carbon magnetic nanoparticles for removal of aniline from aqueous solution: Equilibrium, kinetic and thermodynamic studies, Iran. J. Environ. Health Sci. Eng. 10 (2013) 19–19.
[14] M.A. Khan, Y.-T. Ahn, M. Kumar, W. Lee, B. Min, G. Kim, D.-W. Cho, W.B. Park, B.-H. Jeon, Adsorption studies for the removal of nitrate using modified lignite granular activated carbon, Sep. Sci. Technol. 46 (2011) 2575–2584.
[15] Q. Li, S. Wu, G. Liu, X. Liao, X. Deng, D. Sun, Y. Hu, Y. Huang, Simultaneous biosorption of cadmium(II) and lead(II) ions by pretreated biomass of *Phanerochaete chrysosporium*, Sep. Purif. Technol. 34 (2004) 135–142.
[16] B. Kakavandi, A. Esrafili, A. Mohseni-Bandpi, A. Jonidi Jafari, R. Rezaei Kalantary, Magnetic Fe_3O_4@C nanoparticles as adsorbents for removal of amoxicillin from aqueous solution, Water Sci. Technol. 69 (2014) 147–155.
[17] L.C. Oliveira, R.V. Rios, J.D. Fabris, K. Sapag, V.K. Garg, R.M. Lago, Clay–iron oxide magnetic composites for the adsorption of contaminants in water, Appl. Clay Sci. 22 (2003) 169–177.
[18] Y.-S. Li, J.S. Church, A.L. Woodhead, F. Moussa, Preparation and characterization of silica coated iron oxide magnetic nano-particles, Spectrochim. Acta,Part A. Mol. Biomol. Spectrosc. 76 (2010) 484–489.
[19] I. Langmuir, The adsorption of gases on plane surfaces of glass, mica and platinum, J. Am. Chem. Soc. 40 (1918) 1361–1403.
[20] H. Freundlich, Over the adsorption in solution, J. Phys. Chem. 57 (1906) 385–470.
[21] M. Temkin, V. Pyzhev, Kinetics of ammonia synthesis on promoted iron catalysts, Acta Physiochim. URSS. 12 (1940) 217–222.
[22] S. Lagergren, About the theory of so-called adsorption of soluble substances, K. Sven. Vetenskapsakad. Handl. 24 (1898) 1–39.

[23] Y.-S. Ho, G. McKay, Pseudo-second order model for sorption processes, Process Biochem. 34 (1999) 451–465.
[24] W. Weber, J. Morris, Kinetics of adsorption on carbon from solution, J. Sanit. Eng. Div. Am. Soc. Civ. Eng. 89 (1963) 31–60.
[25] B. Kakavandi, R.R. Kalantary, M. Farzadkia, A.H. Mahvi, A. Esrafili, A. Azari, A.R. Yari, A.B. Javid, Enhanced chromium(VI) removal using activated carbon modified by zero valent iron and silver bimetallic nanoparticles, J. Environ. Health Sci. Eng. 12 (2014) 115.
[26] T. Anirudhan, T.A. Rauf, Adsorption performance of amine functionalized cellulose grafted epichlorohydrin for the removal of nitrate from aqueous solutions, J. Ind. Eng. Chem. 19 (2013) 1659–1667.
[27] S. Nethaji, A. Sivasamy, A. Mandal, Preparation and characterization of corn cob activated carbon coated with nano-sized magnetite particles for the removal of Cr(VI), Bioresour. Technol. 134 (2013) 94–100.
[28] R. Rezaei Kalantary, A. Jonidi Jafari, A. Esrafili, B. Kakavandi, A. Gholizadeh, A. Azari, Optimization and evaluation of reactive dye adsorption on magnetic composite of activated carbon and iron oxide, Desalin. Water Treat. (2015) 1–12.
[29] Z. Han, B. Sani, W. Mrozik, M. Obst, B. Beckingham, H.K. Karapanagioti, D. Werner, Magnetite impregnation effects on the sorbent properties of activated carbons and biochars, Water Res. 70 (2015) 394–403.
[30] M. Balsamo, T. Budinova, A. Erto, A. Lancia, B. Petrova, N. Petrov, B. Tsyntsarski, CO2 adsorption onto synthetic activated carbon: Kinetic, thermodynamic and regeneration studies, Sep. Purif. Technol. 116 (2013) 214–221.
[31] L. Huang, Y. Sun, W. Wang, Q. Yue, T. Yang, Comparative study on characterization of activated carbons prepared by microwave and conventional heating methods and application in removal of oxytetracycline (OTC), Chem. Eng. J. 171 (2011) 1446–1453.
[32] S. Deng, H. Liu, W. Zhou, J. Huang, G. Yu, Mn–Ce oxide as a high-capacity adsorbent for fluoride removal from water, J. Hazard. Mater. 186 (2011) 1360–1366.
[33] Y. Zhang, M. Yang, X.-M. Dou, H. He, D.-S. Wang, Arsenate adsorption on an Fe−Ce bimetal oxide adsorbent: Role of surface properties, Environ. Sci. Technol. 39 (2005) 7246–7253.
[34] Z. Liu, F.-S. Zhang, R. Sasai, Arsenate removal from water using Fe_3O_4-loaded activated carbon prepared from waste biomass, Chem. Eng. J. 160 (2010) 57–62.
[35] N. Öztürk, T.E. Bektaş, Nitrate removal from aqueous solution by adsorption onto various materials, J. Hazard. Mater. 112 (2004) 155–162.
[36] P. Ganesan, R. Kamaraj, S. Vasudevan, Application of isotherm, kinetic and thermodynamic models for the adsorption of nitrate ions on graphene from aqueous solution, J. Taiwan Inst. Chem. Eng. 44 (2013) 808–814.
[37] M.D.G. de Luna, E.D. Flores, D.A.D. Genuino, C.M. Futalan, M.-W. Wan, Adsorption of Eriochrome Black T (EBT) dye using activated carbon prepared from waste rice hulls—Optimization, isotherm and kinetic studies, J. Taiwan Inst. Chem. Eng. 44 (2013) 646–653.
[38] H. Demiral, G. Gündüzoğlu, Removal of nitrate from aqueous solutions by activated carbon prepared from sugar beet bagasse, Bioresour. Technol. 101 (2010) 1675–1680.
[39] D. Wan, H. Liu, R. Liu, J. Qu, S. Li, J. Zhang, Adsorption of nitrate and nitrite from aqueous solution onto calcined (Mg–Al) hydrotalcite of different Mg/Al ratio, Chem. Eng. J. 195–196 (2012) 241–247.
[40] R. Saad, K. Belkacemi, S. Hamoudi, Adsorption of phosphate and nitrate anions on ammonium-functionalized MCM-48: Effects of experimental conditions, J. Colloid Interface Sci. 311 (2007) 375–381.
[41] E. Lacasa, P. Cañizares, J. Llanos, M.A. Rodrigo, Effect of the cathode material on the removal of nitrates by electrolysis in non-chloride media, J. Hazard. Mater. 213–214 (2012) 478–484.
[42] B. Hameed, F. Daud, Adsorption studies of basic dye on activated carbon derived from agricultural waste: *Hevea brasiliensis* seed coat, Chem. Eng. J. 139 (2008) 48–55.
[43] J. Lin, Y. Zhan, Adsorption of humic acid from aqueous solution onto unmodified and surfactant-modified chitosan/zeolite composites, Chem. Eng. J. 200–202 (2012) 202–213.
[44] O.P. Ferreira, S.G. de Moraes, N. Durán, L. Cornejo, O.L. Alves, Evaluation of boron removal from water by hydrotalcite-like compounds, Chemosphere 62 (2006) 80–88.
[45] N. Yang, S. Zhu, D. Zhang, S. Xu, Synthesis and properties of magnetic Fe_3O_4-activated carbon nanocomposite particles for dye removal, Mater. Lett. 62 (2008) 645–647.
[46] H.Y. Zhu, Y.Q. Fu, R. Jiang, J.H. Jiang, L. Xiao, G.-M. Zeng, S.L. Zhao, Y. Wang, Adsorption removal of congo red onto magnetic cellulose/Fe_3O_4/activated carbon composite: Equilibrium, kinetic and thermodynamic studies, Chem. Eng. J. 173 (2011) 494–502.